RSC Advances

PAPER

View Article Online
View Journal | View Issue

Cite this: *RSC Adv.*, 2023, **13**, 29809

Enhanced degradation of ibuprofen in an integrated constructed wetland-microbial fuel cell: treatment efficiency, electrochemical characterization, and microbial community dynamics

Youssef A. Youssef,[a] Mohamed E. Abuarab,[a] Ahmed Mahrous[a] and Mohamed Mahmoud *[b]

Over the past few decades, there has been a growing concern regarding the fate and transport of pharmaceuticals, particularly antibiotics, as emerging contaminants in the environment. It has been proposed that the presence of antibiotics at concentrations typically found in wastewater can impact the dynamics of bacterial populations and facilitate the spread of antibiotic resistance. The efficiency of currently-used wastewater treatment technologies in eliminating pharmaceuticals is often insufficient, resulting in the release of low concentrations of these compounds into the environment. In this study, we addressed these challenges by evaluating how different influent ibuprofen (IBU) concentrations influenced the efficiency of a laboratory-scale, integrated constructed wetland-microbial fuel cell (CW-MFC) system seeded with *Eichhornia crassipes*, in terms of organic matter removal, electricity generation, and change of bacterial community structure compared to unplanted, sediment MFC (S-MFC) and abiotic S-MFC (AS-MFC). We observed that the addition of IBU (5 mg L^{-1}) resulted in a notable decrease in chemical oxygen demand (COD) and electricity generation, suggesting that high influent IBU concentrations caused partial inhibition for the electroactive microbial community due to its complexity and aromaticity. However, CW-MFC could recover from IBU inhibition after an acclimation period compared to unplanted S-MFC, even though the influent IBU level was increased up to 20 mg L^{-1}, suggesting that plants in CW-MFCs have a beneficial role in relieving the inhibition of anode respiration due to the presence of high levels of IBU; thus, promoting the metabolic activity of the electroactive microbial community. Similarly, IBU removal efficiency for CW-MFC (*i.e.*, 49–62%) was much higher compared to SMFC (*i.e.*, 29–42%), and AS-MFC (*i.e.*, 20–22%) during all experimental phases. In addition, our high throughput sequencing revealed that the high performance of CW-MFCs compared to S-MFC was associated with increasing the relative abundances of several microbial groups that are closely affiliated with anode respiration and organic matter fermentation. In summary, our results show that the CW-MFC system demonstrates suitability for high removal efficiency of IBU and effective electricity generation.

Received 22nd August 2023
Accepted 6th October 2023

DOI: 10.1039/d3ra05729a

rsc.li/rsc-advances

1. Introduction

Over the past few years, contaminants of emerging concern (CECs), including pesticides and endocrine-disrupting chemicals, have gained increased attention as a result of their ubiquitous presence in the environment and harmful ecological impacts, such as the prevalence of antibiotic resistance genes.[1–3] Antibiotics – which have been used to cure and prevent illnesses, and foster animal growth – are among the most often identified CECs in water and soil, with residues ranging from ppb to ppm.[4,5] For instance, approximately 50 000 tons of antibiotics are discharged into the aquatic environment in China annually.[6] Recent studies revealed that wastewater treatment facilities have a crucial role in spreading CECs in receiving environments since conventional biological wastewater treatment technologies are inefficient enough to remove CECs.[7–9]

Ibuprofen (IBU), which is a class of non-steroidal anti-inflammatory medications, is one of the most commonly used drugs globally, with acute toxicity to aquatic vertebrates and invertebrates.[10,11] Among various CECs, IBU is often detected in

[a]*Agricultural Engineering Department, Faculty of Agriculture, Cairo University, Giza 12613, Egypt*

[b]*Water Pollution Research Department, National Research Centre, 33 El-Buhouth St., Dokki, Cairo 12311, Egypt. E-mail: moh.mahmoud@nrc.sci.eg*

the effluent of domestic wastewater treatment plants (WWTPs) at relatively high concentrations (*i.e.*, up to 1.7 mg L^{-1}),[12] which is much higher than other analgesic and anti-inflammatory drugs in various European Union countries.[13] In addition, emerging IBU contamination in wastewater would change the structure and function of microbial communities in WWTPs, limiting organic matter and nitrogen biodegradation and removal.[14]

Due to antibiotics' substantial presence and high bioaccumulation capability in aquatic environments, several advanced oxidation technologies, including Fenton, UV–H_2O_2, ozone, and electrochemical-based oxidation, have been extensively proposed to remove them from different waste streams.[15–18] However, due to the high cost and limited selectivity of the advanced oxidation processes, advanced biological wastewater treatment technologies have gained more attention for antibiotic breakdown.[19–21] Although currently used biological WWTPs (such as membrane bioreactors and conventional activated sludge) exhibit high efficiency (*i.e.*, >70%) for removing targeted antibiotics (*e.g.*, ciprofloxacin, oxytetracycline, and sulfamethazine) from municipal wastewater,[22] their reliance on using oxygen or air as electron acceptors increases their complexity as well as operation and maintenance (O&M) costs, limiting their implementation in resource-limited communities.[23] Thus, there is an urgent need to develop economical, easy-to-implement treatment technologies to control the release of antibiotics into environmental ecosystems.

Among several advanced biological wastewater treatment technologies, constructed wetlands (CWs) have emerged as a sustainable, economical approach for removing residual contaminants, including CECs, from municipal wastewater owing to their simple design, relatively cheap O&M cost, low energy demand, and easy management.[24] Additionally, CWs could improve the microclimate of urban cities, lower air pollution, and eliminate potential odors as compared to commonly used wastewater treatment technologies.[25,26] For instance, Deng *et al.*[27] observed that CWs were effective in removing up to 89% of trimethoprim and 61% of sulfamethoxazole from aquaculture wastewater containing antibiotics. However, due to their relatively large footprint, sluggish contaminate degradation efficiency, and partial inhibition of functional microbial communities, conventional CWs have always been confined to practical applications for antibiotic removal, especially in urban and semi-urban regions.[28] Significant progress has been made in the design and operation of CWs to promote the transformation and removal efficiency of antibiotics, including aeration, multi-stage configuration, and connecting multiple CWs in series.[29–31]

Among these modified CWs, the integration of CWs with microbial fuel cells (MFCs) holds promising prospects owing to their advantages in promoting contaminants degradation through regulated electron transfer to conductive electrodes, the remarkable reduction of greenhouse gas emissions, and the capability to produce renewable energy (*i.e.*, electricity).[32] CW-MFCs are frequently used to treat different waste streams, including municipal wastewater and azo dye-containing wastewater treatment. Although CW-MFCs seem a promising option for wastewater treatment, there are still some practical obstacles to be overcome, such as low biorefractory organics matter removal efficiency, low electric current output, and high internal resistance.[33] Recently, several studies reported that the integration of CWs and MFCs remarkably improved antibiotic biodegradation efficiency.[34] In a typical CW-MFC, implanting inexhaustible conductive electrodes, which act as electron acceptors and electron donors, would tune the redox chemistry in their vicinity, regulating the microbial activity and enhancing electron transfer and destruction efficiencies of CECs.[35] In addition, the continuous flow of metabolically-produced electrons from organic matter biodegradation inhibits their buildup, avoiding the formation of a highly reductive environment that promotes methanogens.[36] Thus, the integrated CW-MFC technology seems to be an effective and environmentally friendly approach for controlling and preventing antibiotic prevalence in the aquatic environment.

Although electricity generation under antibiotic stress has been extensively studied in CW-MFC and IBU is expected to cause a deleterious impact on the composition and richness of the microbial community population, it was unclear how variable IBU concentrations influenced the electricity production and microbial community structure, especially electroactive bacteria (EAB). Furthermore, IBU removal seems to occur mostly by microbial biodegradation,[37] and the significance of functional microbial community in IBU elimination in this system remains poorly explored. In this study, we addressed these challenges by evaluating the IBU removal efficiency and electricity generation attained by a laboratory-scale CW-MFC system seeded with *Eichhornia crassipes* compared to unplanted, sediment MFC (S-MFC) and abiotic S-MFC (AS-MFC). In addition, the degradation mechanism of IBU was identified. High-throughput sequencing was also used to examine the anodic microbial community structures of the CW-MFC and S-MFC systems. Finally, by combining different analyses, we elucidated the potential biodegradation pathway of IBU in CW-MFC.

2. Material and methods

2.1. Reactor setup and operating conditions

We used three identical reactors, which were made of plexiglass with an inner diameter of 11.4 cm, a height of 22.5 cm, and an effective volume of 2 L, with the same configurations: (1) R1 (*i.e.*, CW-MFC system seeded with *Eichhornia crassipes*), (2) R2 (*i.e.*, biotic sediment unplanted MFC (S-MFC)), and R3 (abiotic S-MFC (AS-MFC)) (Fig. 1). Each reactor was filled (from bottom to up) with a 2 cm layer of gravel (3–6 mm in diameter), 3.5 cm of granular activated carbon (GAC) anode/stainless steel mesh (grade 304), 5 cm of gravel, and 3.5 cm of GAC/stainless steel mesh cathode. We chose stainless steel mesh as a current collector owing to its highly exposed surface area, and outstanding corrosion-resistive and electrical conductivity properties. In this configuration, the distance between the anode and cathode electrodes was kept constant at ~5 cm. The projected surface area of both electrodes was ~102 cm^2. Anode

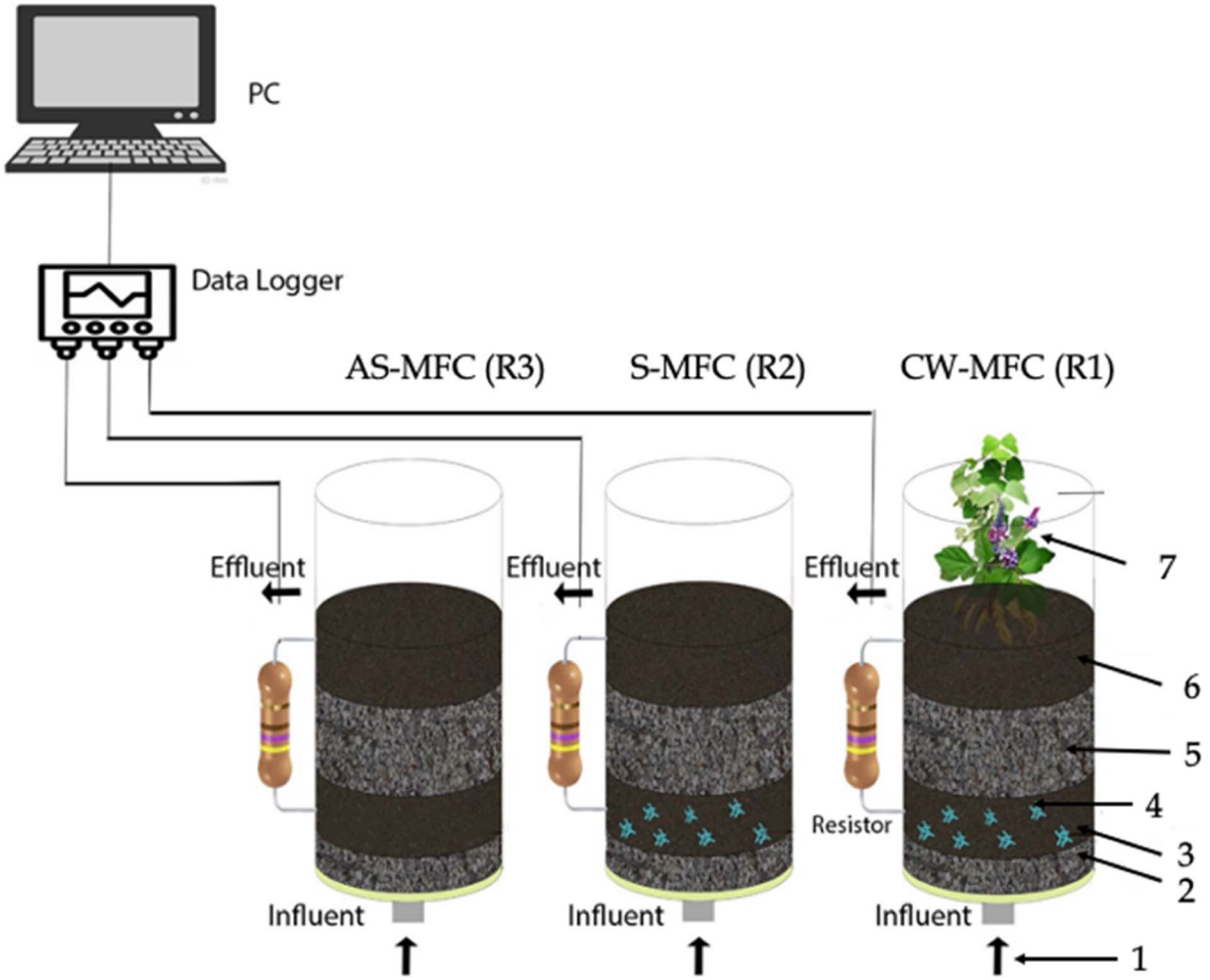

Fig. 1 Schematic diagram of three reactors used in this study. ((1) Influent pumping; (2) gravel; (3) stainless-steel-GAC anode; (4) electroactive biofilm; (5) gravel; (6) stainless-steel-GAC cathode; (7) *Eichhornia crassipes*).

and cathode electrodes were electrically connected through copper wires with an external resistance (R_{ext}) of 1500 Ω.

Prior to reactors start-up, we inoculated them with 0.5 L of aerobic sludge collected from the Zenin wastewater treatment plant in Cairo, Egypt, and the reactors were fed with 15 mM acetate medium (*i.e.*, chemical oxygen demand (COD) = 1.2 ± 0.2 g L^{-1}) as described elsewhere.[38] In order to inhibit the proliferation of algae, all reactors were covered by aluminum foil to prevent the penetration of light. The reactors were semi-continuously operated at a hydraulic retention time (HRT) of 3 days, a hydraulic loading rate (HLR) of 64.70 L m^{-2} d^{-1}, and an organic loading rate (OLR) of 0.63 kg COD per m^3 per day. Our research study was structured into four discrete phases, denoted as phase I, at which reactors were fed with a 15 mM acetate medium. In phase II, 5 mg L^{-1} of IBU (≥98%; Sigma-Aldrich Chemie, Steinheim, Germany) was spiked to acetate medium. Finally, the IBU concentration in the influent was gradually increased to 10 mg L^{-1} (phase III) and 20 mg L^{-1} (phase IV). We performed all experiments using two independent reactors at room temperature (28 ± 3 °C).

2.2. Chemical and electrochemical analysis

We regularly measured pH and COD concentrations according to the method described in the Standard Methods for the Examination of Water and Wastewater,[39] and estimated the COD removal efficiency using the following relationship:[40,41]

$$\text{COD removal}(\%) = \frac{\text{COD}_{\text{influent}} - \text{COD}_{\text{effluent}}}{\text{COD}_{\text{influent}}} \times 100 \quad (1)$$

where $\text{COD}_{\text{influent}}$ is the COD concentration to the reactor (expressed as mg COD per L) and $\text{COD}_{\text{effluent}}$ is the residual COD concentration (expressed as mg COD per L).

We measured the IBU concentrations in influent and treated effluent using Ultra-Performance Liquid Chromatography (UPLC) (Ultimate 3000, Thermo Scientific, USA) equipped with a C18 column (Acquity UPLC BEH HILIC Column, Waters, Milford, MA, USA; 1.7 μm, 2.1 × 150 mm) and a diode array detector after filtering them through 0.22 μm membrane filters. The mobile phase was a mixture of acetonitrile and DI water (70 : 30, v/v) at a flow rate of 0.3 mL min^{-1} and the injection volume was 5 μL. For plant tissues, we extracted IBU by the

ultrasonication of tissues in a mixture of methanol:acetone (95 : 5, v/v) according to the method described in Zhang *et al.*[42]. Then, the extract was further cleaned up with activated carbon prior to the UPLC injection.

We monitored the close-circuit reactors' potential across a fixed external resistance of 1500 Ω using a data acquisition system (National Instruments, USA) connected to a personal computer. At the end of each operating phase, polarization experiments were conducted by changing the external resistances from 0.1 to 55 kΩ, and the corresponding voltage and current values were monitored for 25 minutes at each external resistance. The current and power were estimated according to Ohm's law, and the current and power densities were calculated by normalizing the current and power to the reactor's effective volume, respectively. We estimated the estimation of coulombic efficiency (CE) as described elsewhere by normalizing the recovered electrons as current to the overall COD removed[43] (eqn (2)).

$$\mathrm{CE} = \frac{M \int_0^t I \mathrm{d}t}{nVF\left(\mathrm{COD}_{\mathrm{inf}} - \mathrm{COD}_{\mathrm{eff}}\right)} \quad (2)$$

where M is the oxygen molecular weight, I is current output (A), F is Faraday's constant (96 485 C mol^{-1}), n is the number of electrons exchanged per mol of oxygen, and V is the anode chamber volume.

2.3. Microbial community and bioinformatics analysis

Biofilm samples from CW-MFC and S-MFC bioanodes were collected into a 50 mL sterile centrifuge tube having DNA–free phosphate buffer, which were subsequently centrifuged at 10 000 rpm for 15 min. Then, the genomic DNA was extracted using a Qiagen DNA isolation kit (Hilden, Germany) according to the manufacturer's instructions. We determined the quantity and quality of extracted DNA samples using a NanoDrop spectrophotometer (Thermo Scientific, USA). Finally, high-throughput microbial community analysis was performed using a MiSeq Illumina sequencer (Illumina Inc., USA) using the bar-coded primer set following the manufacturer's guidelines as described elsewhere.[40] We performed taxonomic classification using Python scripts in QIIME software as described elsewhere.[44]

2.4. Statistical analysis

We performed a one-way ANOVA statistical analysis using IBM SPSS Statistics for Windows, Version 25.0 (Armonk, NY: IBM Corp), considering p-values less than 0.05 statistically significant.

3. Results and discussion

3.1. Electricity production and responses of electroactive bacteria to ibuprofen

Following the successful formation of EAB biofilm (data not shown), we fed the CW-MFC and S-MFC with ibuprofen-containing synthetic wastewater. Their performance was evaluated by monitoring the variation in potential generated over time during semi-continuous operation for four consecutive cycles (Fig. 2a). For both systems, we observed that the potential steadily increased, peaking on the second day of each semi-continuous cycle, which was followed by a subsequent decrease at the end of each cycle. For instance, in phase I, CW-MFC showed a relatively higher maximum closed-circuit potential output than S-MFC (0.17 ± 0.03 V *versus* 0.11 ± 0.02 V), implying that the presence of the plant in CW-MFC significantly enhances the substrate uptake, and, hence, the electricity generation.[45,46] Upon introducing IBU at a final concentration of 5 mg L^{-1} (*i.e.*, phase II), both systems exhibited slightly lower electricity generation, with CW-MFC generating a 1.21-fold higher potential output compared to S-MFC. The lower potential output regardless of the presence or absence of plants in our systems suggests that IBU partially impaired the metabolic activity of EAB biofilm.[37] Interestingly, a further increase in the influent IBU concentration to 10 mg L^{-1} induced the metabolic activity of EAB biofilm in CW-MFC, resulting in a remarkable increase in maximum potential output (*i.e.*, 0.21 ± 0.02 V), which is ∼1.5-fold higher than that of S-MFC (*i.e.*, 0.14 ± 0.04 V). In phase IV, we observed a slight decrease in the average maximum potential output in both CW-MFC and S-MFC systems. The most likely reason for relatively lower CW-MFC and S-MFC performance with high influent IBU concentrations was the partial inhibition caused by its complexity and aromaticity. These results are in agreement with previous studies (Table 1), suggesting that plants in CW-MFCs have a beneficial role in relieving the inhibition of anode respiration due to the presence of high levels of antibiotics (*e.g.*, IBU); thus, promoting the metabolic activity of the EAB community[47,48]

Similar to the potential profile, we observed that CW-MFCs exhibited higher COD removal efficiency for the entire experimental phases compared to S-MFCs with statistically significant disparities ($p < 0.05$) in all experimental phases (Fig. 2b). For instance, CW-MFC demonstrated a COD removal efficiency of 81 ± 7% compared to only 61 ± 5% for S-MFC when 5 mg per L IBU medium was used as an influent, confirming the beneficial role of *Eichhornia crassipes* in improving the substrate uptake rate and relieving the inhibition due to the presence of IBU. In addition, we observed that AS-MFC demonstrated a low COD removal efficiency of ∼30%. We also estimated the coulombic efficiencies (CE) for CW-MFCs and S-MFCs during all experimental phases, which represents a crucial parameter for quantifying the conversion of electrons from the organic matter biodegradation. In phase I, we observed 1.67 ± 0.12% and 0.85 ± 0.14% of electrons were recovered as electric current for CW-MFCs and S-MFCs, respectively. Further increase in the influent IBU concentration to 5 mg L^{-1} resulted in a remarkable decrease in CE values for CW-MFC (0.99 ± 0.11%) and S-MFC (0.45 ± 0.05%). For phase III, the CE value for CW-MFC was increased to 1.92 ± 0.14%, which was in agreement with the potential profile, while the CE value for S-MFC remained relatively low (0.47 ± 0.09%). Generally, our results reveal that the presence of the plant in CW-MFC resulted in superior electricity generation and electron recovery rate compared to S-MFC across varying influent IBU loads, implying that the increase in concentrations of IBU did not have a significant impact on

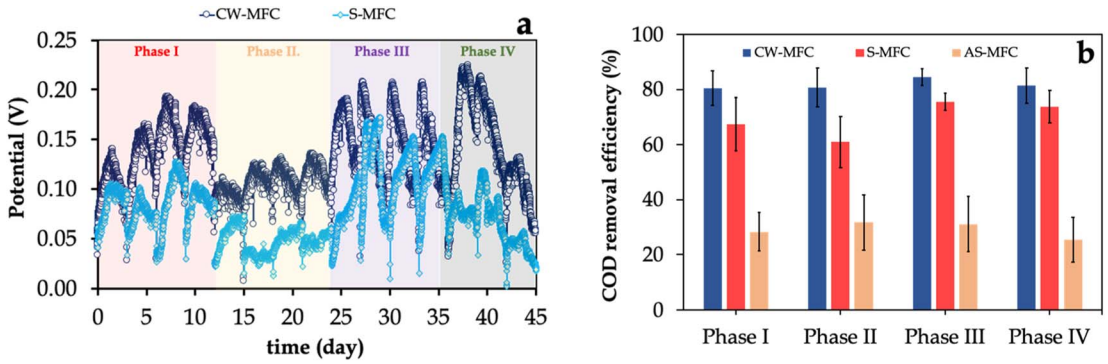

Fig. 2 (a) The potential output of CW-MFC and S-MFC fed with different IBU concentrations. (b) COD removal efficiencies in CW-MFC, S-MFC, and AS-MFC. The values represent the mean of replicates, while the error bars correspond to the standard deviations ($n = 3$).

Table 1 Summary of constructed wetland-microbial fuel cell (CW-MFC) performance fed with antibiotics

Antibiotic used	Co-substrate	Anode	Cathode	Wetland plant	Mode of operation	Wastewater treatment efficiency	Maximum power density	Reference
Sulfadiazine (SDZ)	Glucose	Mn ore	Carbon fiber	*Acorus calamus*	Continuous	68%	~5.1 mW m^{-2}	7
Diclofenac (DCF)	Synthetic hospital wastewater	Graphite plates	Graphite plates	*Eichhornia crassipes*	Continuous	~78% removal efficiency of DCF	26 mW m^{-2}	35
Sulfadiazine (SDZ)	Glucose	Carbon cloth–graphite	Carbon cloth–graphite	*Acorus calamus*	Batch	86% removal efficiency of SDZ	2.55 mW m^{-2}	50
Sulfamethoxazole (SMX)	Glucose	Titanium mesh box	Titanium mesh	*Iris tectorum* Maxim.	Continuous	82.37% removal efficiency of SMX	7.43 mW m^{-2}	51
Sulfadiazine (SDZ)	Glucose	Mn ore	Carbon fibre felt	*Acorus calamus*	Continuous	60.5% removal efficiency of SDZ	9.70 mW m^{-2}	52
Ciprofloxacin (CIP)	Glucose	Iron–carbon particles	Carbon electrode	*Iris tectorum*	Continuous	91.2% removal efficiency of CIP	3.55 mW m^{-2}	53
Tetracycline (TC)	Glucose	GAC	GAC	*Canna indica*	Semi-continuous	99.2% removal efficiency of TC	123.4 mW m^{-3}	54
Ibuprofen (IBU)	Acetate	GAC	GAC	*Eichhornia crassipes*	Semi-continuous	54% removal efficiency of IBU	8.9 mW m^{-2}	This study

electricity generation and COD removal. The likely reason for this observation is that the presence of plants in CW-MFCs favors EAB metabolic activity for higher organic matter biodegradation and/or the ability of EAB to utilize acetate as a co-substrate for carbon assimilation. Notably, the potential output generated and CE in phase II was observed to be lower compared to phase III, even though COD removal in phase II was comparable with that of phase III. These findings suggest that the IBU likely hindered the microbial activity within the CW-MFC and S-MFC, which required an acclimation period to recover the high metabolic activity of the electroactive microbial community.[49]

The polarization and power curves in Fig. 3 illustrate the electricity generation efficiency of CW-MFC and S-MFC fed with influent IBU concentrations. Consistent with the potential output profile (Fig. 2a), CW-MFC fed with 10 mg per L IBU-containing synthetic wastewater exhibited the highest maximum power density of 8.9 ± 0.12 mW m^{-3}, which is 2.6-fold higher than S-MFC fed with the same influent IBU concentration (3.4 ± 0.14 mW m^{-3}) (Fig. 3a). Regardless of the influent IBU concentration, CW-MFCs always had much higher maximum power density (*i.e.*, 1.75–2.60-fold) compared to S-MFCs. In order to conduct a more comprehensive analysis of the electricity generation capabilities of CW-MFCs and S-MFCs under varying influent conditions, the internal resistances of the CW-MFCs and S-MFCs were estimated by calculating the slopes derived from linear regression analysis of select data points within the ohmic polarization region of the polarization curves (Fig. 3b). Despite the fact that CW-MFCs exhibited higher potential output and power densities compared to S-MFC-CW, we did not observe any statistically significant disparities observed in the average internal resistances in the internal resistances between CW-MFCs and S-MFCs in phase I. For instance, the internal resistance was 830 ± 10 Ω for CW-MFCs and 890 ± 30 Ω for S-MFCs ($p > 0.05$). However, increasing the influent IBU concentrations resulted in decreasing the internal resistances of planted CW-MFCs compared to unplanted S-MFCs, especially for phase III (*i.e.*, 610 ± 30 Ω for CW-MFCs and 840 ± 34 Ω for S-MFCs) ($p < 0.05$).

In our study, we observed that the electricity generation performance of CW-MFCs was improved in all experimental phases, as evidenced by the increased potential output, power

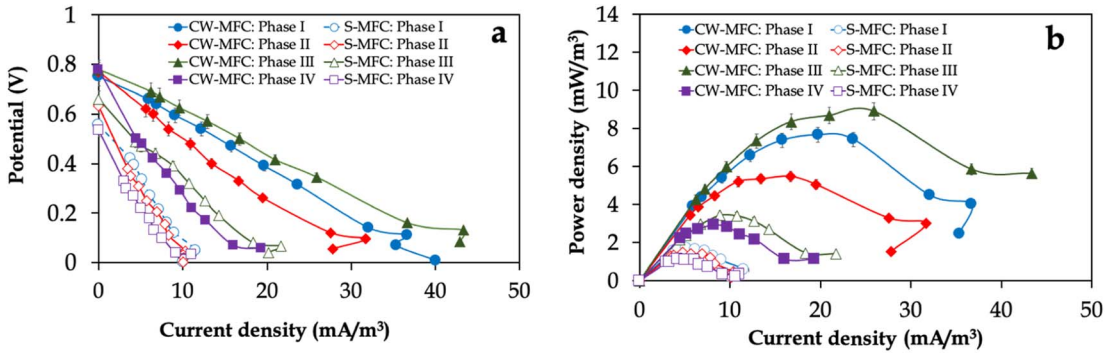

Fig. 3 (a) Power density and (b) polarization curves of CW-MFC and S-MFC fed with different IBU concentrations.

density, COE removal, and CE. *Eichhornia crassipes* species was employed as a macrophyte due to its robust root system, which facilitated increased dissolved oxygen production and the generation of rhizodeposition substrates. Previous studies suggested that the presence of plants in the cathode of CW-MFCs resulted in an elevation of dissolved oxygen concentration. This increase in dissolved oxygen concentration facilitated the following reaction: $6O_2 + 24H^+ + 24e^- \rightarrow 12H_2O$, thereby expediting the cathode half-cell potential as well as the overall cell reaction and potential output.[45–47,55] More importantly, a recent study revealed that the presence of plants in CW-MFCs promotes the prevalence of EAB (such as *Geobacteraceae*) that colonize the anode surface.[56] In addition, the introduction of rhizodeposition substrates has the potential to enhance the electroactive microbial community's biodiversity,[57] improving the performance of electricity generation of CW-MFCs.

3.2. Ibuprofen removal efficiency and its accumulation in electrode layers and plant tissues

Fig. 4 illustrates the IBU removal efficiencies in CW-MFC, S-MFC, and AS-MFC fed with different influent IBU concentrations. We observed that the influent IBU concentrations for CW-MFC and S-MFC showed a rapid decrease within the first 24 hours, followed by a gradual decrease until the end of each operating cycle. Interestingly, CW-MFCs exhibited superior IBU removal efficiencies and removal rates compared to S-MFC,

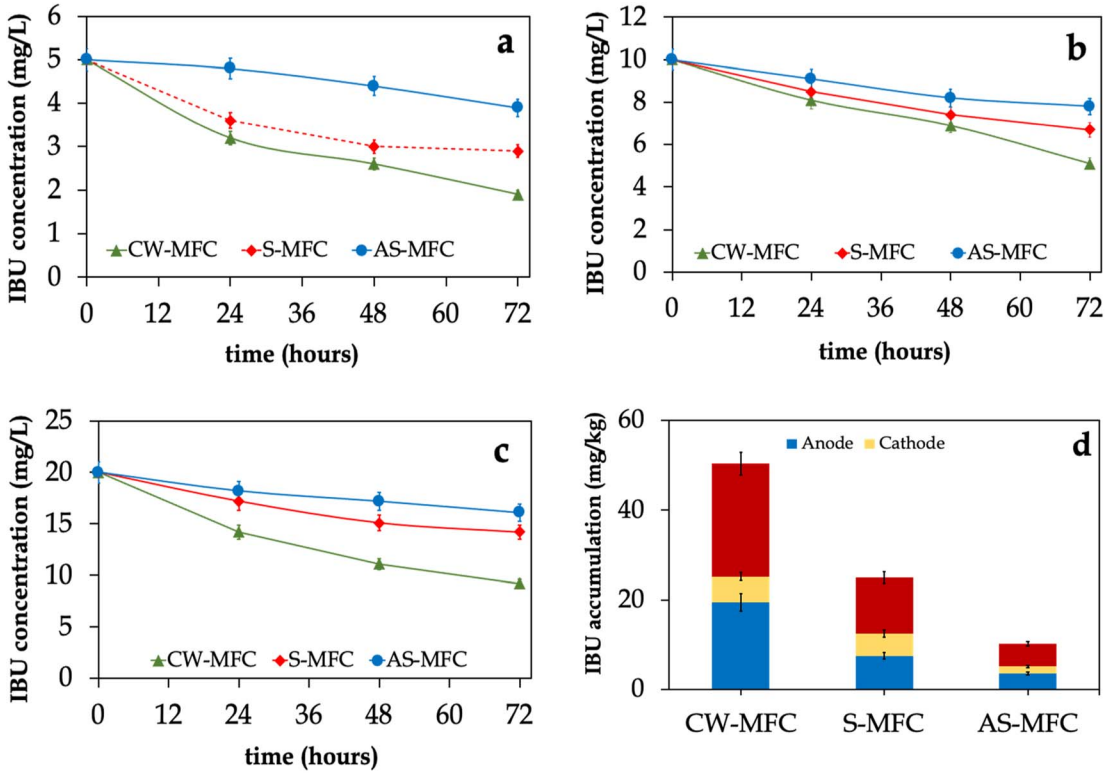

Fig. 4 Effluent concentrations of IBU of CW-MFCs, S-MFCs, and AS-MFCs fed with different influent IBU concentrations: (a) 5 mg per L IBU, (b) 10 mg per L IBU, and (c) 20 mg per L IBU. (d) IBU accumulation in the anode and cathode layers of CW-MFCs, S-MFCs, and AS-MFCs. The values represent the mean of replicates, while the error bars correspond to the standard deviations ($n = 3$).

especially in phases III and IV ($p < 0.05$). On the other hand, we observed approximately 20% of IBU removed in AS-MFC, which could be attributed to pollutant adsorption on the GAC surface, plant uptake, or both. The most likely reason for having a higher IBU removal efficiency in CW-MFC compared to S-MFC and AS-MFC might be due to the release of oxygen from plant roots, which potentially offsets the chemical and biological utilization of oxygen by rhizosphere microbes.[58] Several plant species have the capability to produce oxygen in the vicinity of their roots on a continuous basis, and the rates at which oxygen is released vary among different species.[55] In this context, the released oxygen has the capacity to support the chemical degradation of pollutants found in wastewater, resulting in favoring the growth of aerobic microbes within the rhizosphere area and enhancing wastewater treatment efficiency.[59,60]

In order to elucidate the removal mechanism of IBU, we evaluated the accumulation of IBU on granular activated carbon as well as in plant tissues at the end of phase IV. Nevertheless, the concentrations of IBU in plant tissues were found to be below the detectable limit. Hence, the present description solely pertains to the accumulation of IBU within the electrode layers. According to the data presented in Fig. 4d, CW-MFC demonstrated a statistically significant increase in total IBU residues (combined anode and cathode layers) compared to the S-MFC and AS-MFC ($p < 0.05$). The concentrations of IBU residues in the CW-MFC, S-MFC, and AS-MFC were determined to be 25.2 ± 0.9, 12.5 ± 0.8, and 5.1 ± 0.4, mg kg^{-1}, respectively. In addition, the average IBU residues in the anode layers were found to be 30–70% higher than those in the cathode layers. Collectively, our results strongly demonstrate that the presence of the plant improved the accumulation of IBU in the electrode layers of CW-MFC, resulting in much higher IBU removal efficiency.

The main mechanisms involved in the removal of antibiotics, such as IBU, in constructed wetlands are a combination of pollutant adsorption, plant uptake, and degradation processes (*e.g.*, photodegradation and biological degradation).[61] Although the photodegradation of IBU through photochemical processes may serve as a significant pathway for its removal,[62] we rule out its contribution in our experimental setup owing to our use of aluminum foil to prevent the penetration of light. Furthermore, it was observed that IBU exhibited resistance to hydrolysis, with significantly low hydrolysis rates at a neutral pH (*i.e.*, ~7.0).[63] In contrast to S-MFC and AS-MFC, CW-MFCs offer a notable advantage to promote continuous biological degradation of substrates using electroactive microbial communities to directly generate electric current by respiring the resulting electrons into inexhaustible electron acceptors (*i.e.*, anode surface). In the presence of co-substrates (*i.e.*, acetate in our case), the electroactive microbial communities consume them as a carbon or energy source, indirectly facilitating the biodegradation of hardly-degradable substrates (*e.g.*, antibiotics).[64] Hence, the primary cause for the IBU degradation in CW-MFC in our study can be attributed primarily to organic substrate adsorption and biodegradation, implying the important role of plants in relieving antibiotic toxicity in CW-MFCs. However, the direct uptake of IBU by plants seems to have a minimal impact on the overall IBU removal as we only detected trivial IBU levels in plant tissues. Hence, we deduced that the beneficial impact of the plant primarily arises from its indirect influence, including the facilitation of biological degradation within the rhizosphere zone, the elevation of cathode potential in CW-MFC due to the increased dissolved oxygen concentration, and the enhancement of anodic microbiome structure and biodiversity, which, in turn, result in expediting the metabolic activity of EAB biofilm.[57,65–67]

To the best of our knowledge, there has been a lack of scholarly literature documenting the impact of plants on the accumulation of IBU in CW-MFCs. However, our study suggests that the inclusion of plants significantly contributes to the proliferation of diverse electroactive microbiomes that colonize the anode surface, which, in turn, enhances the electrosorption capability of anodic biofilm in the elimination of antibiotics (*e.g.*, IBU).[68] Recently, Kong *et al.*[69] documented that the movement of charged and polar molecules toward the granular activated carbon electrode resulted in the formation of a double electric layer, facilitating the electrosorption capacity of sulfadiazine. In another study, Yang *et al.*[70] demonstrated that MFCs can effectively drive an electrosorption system, thereby enhancing the degradation of tetracycline. In addition, the antibiotic's direct uptake by plants in CW-MFCs is strongly influenced by the physicochemical properties of antibiotics (such as hydrophobicity and antibiotic solubility) and specific characteristics of the used plant species.[47] Given that IBU is a hydrophobic compound, with a logarithm octanol–water partition coefficient (K_{ow}) of 2.48,[71] the direct uptake of IBU by plants seems to be trivial owing to the transpiration limitations,[72] which is in agreement with our results. The lack of IBU detection in plant tissues may be attributed to its potential degradation *via* glycosylation and glutathione pathways.[73]

3.3. Microbial community analysis

At the end of phase IV, we harvested the anodic biofilm-covered GAC anodes in CW-MFCs and S-MFCs systems, and performed high-throughput sequencing of the V4 region in the 16S rRNA gene of anodic biofilm. We observed that a significant proportion of bacterial 16S rRNA genes were found to be affiliated with six phyla: *Proteobacteria*, *Bacteroidota*, *Desulfobacterota*, *Firmicutes*, *Chloroflexi*, and *Actinobacteriota* (Fig. 5a), which is in agreement with findings reported in previous studies.[74] Many phylotypes of phyla *Bacteroidota*, *Firmicutes*, *Actinobacteria*, and *Chloroflexi* have been identified as capable of fermenting sugars, while several members of the phylum Proteobacteria have been identified for performing anode respiration.[44,75,76] The higher abundance of electroactive Proteobacteria phylum in CW-MFCs anodic biofilm compared to S-MFCs agrees with our previous results, confirming that the presence of plants in CW-MFCs favors EAB metabolic activity for higher organic matter biodegradation and electricity generation. Within the phylum Proteobacteria, the *Gammaproteobacteria* subgroup exhibited the highest relative abundance, especially for CW-MFC anodic biofilm compared to S-MFC and inoculum. In addition, we observed that the other dominant classes included *Desulfuromonadia* and *Bacteroidia* (Fig. 5b). Several members of

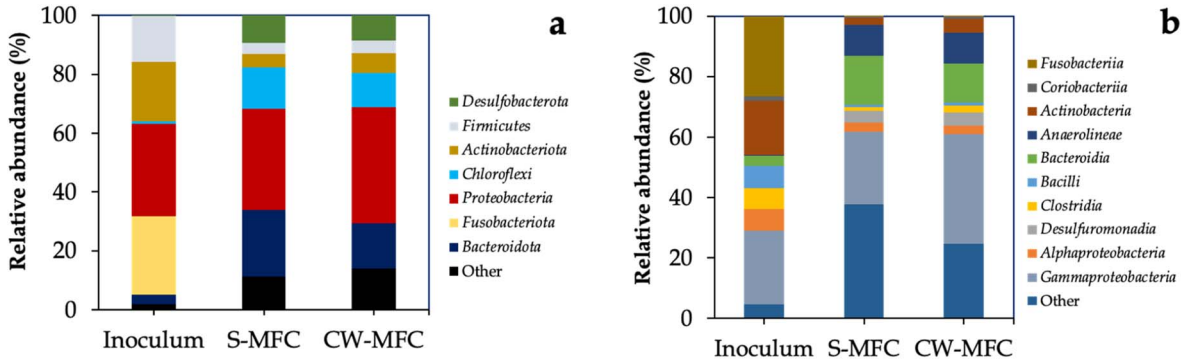

Fig. 5 Bacterial community sequencing results (a) at the phylum level and (b) at the class level. Phylotypes < 2% of total sequences are grouped as "others".

those classes are known for being EAB and have been detected in different bioelectrochemical systems.[77,78]

4. Conclusion

The potential risks to public health and environmental ecosystems caused by antibiotics are potentially more severe in comparison to those caused by biodegradable organic pollutants and nitrogen. Generally, biodegradable organic pollutants (*e.g.*, carbohydrates and protein), which have low toxicity and a high biodegradation rate, are commonly used as a co-substrate to promote the destruction of recalcitrant organic pollutants, including antibiotics. This study provides evidence that the incorporation of *Eichhornia crassipes* species significantly enhances the efficiency of removing IBU in a semi-continuous-operated CW-MFC. Although electricity generation under antibiotic stress has been extensively studied in CW-MFC and IBU is expected to cause a deleterious influence on the composition and richness of the microbial community population, it was unclear how variable IBU concentrations influenced the electricity production and microbial community structure, especially electroactive bacteria (EAB). Compared to S-MFC and AS-MFC, the CW-MFC fed with IBU-containing synthetic wastewater exhibited higher COD removal, electricity generation, and CE even at high influent IBU (*i.e.*, up to 20 mg L^{-1}), confirming the beneficial role of *Eichhornia crassipes* in improving the substrate uptake rate and relieving the inhibition due to the presence of IBU. In addition, we observed that CW-MFCs exhibited superior rates for IBU removal compared to S-MFC, especially in phases III and IV, with approximately 20% of IBU being removed due to pollutant adsorption on the GAC surface. The likely reason for having a higher IBU removal efficiency in CW-MFC compared to S-MFC and AS-MFC might be due to the release of oxygen from plant roots, which potentially offsets the chemical and biological utilization of oxygen by rhizosphere microbes. More importantly, high throughput sequencing reveals that the presence of plants in CW-MFCs promotes the prevalence of EAB that colonize the anode surface, resulting in enhancing the electroactive microbial community's biodiversity and improving the overall performance of CW-MFCs for IBU removal and electricity generation.

Author contributions

Y. A. Y.: methodology, formal analysis, investigation, visualization, writing – original draft. M. E. A.: conceptualization, formal analysis, writing – review & editing, supervision, resources, funding acquisition. A. M.: writing – review & editing, supervision. M. M.: conceptualization, formal analysis, investigation, visualization, writing – review & editing, supervision, project administration, resources, funding acquisition.

Conflicts of interest

The authors declare no competing interests.

Acknowledgements

This study was funded by the Science, Technology, and Innovation Funding Authority (STDF), Egypt (grant no. 33445).

References

1 R. Rafieenia, M. Sulonen, M. Mahmoud, F. El-Gohary and C. A. Rossa, *Sci. Total Environ.*, 2022, 153923.
2 X. Yi, N. H. Tran, T. Yin, Y. He and K. Y.-H. Gin, *Water Res.*, 2017, **121**, 46–60.
3 S. Chauhan, A. Yadav, P. M. Kurup, X. Li, P. Swarnakar and R. K. Gupta, *RSC Sustainability*, 2023, **1**, 418–431.
4 R. Rafieenia, M. Mahmoud, F. El-Gohary and C. A. Rossa, *Sustain. Energy Technol. Assessments*, 2022, **54**, 102805.
5 H. Wen, H. Zhu, B. Yan, Y. Xu and B. Shutes, *Chemosphere*, 2020, **250**, 126252.
6 Q.-Q. Zhang, G.-G. Ying, C.-G. Pan, Y.-S. Liu and J.-L. Zhao, *Environ. Sci. Technol.*, 2015, **49**, 6772–6782.
7 H. Li, H. Cao, T. Li, Z. He, J. Zhao, Y. Zhang and H.-L. Song, *J. Hazard. Mater.*, 2023, **460**, 132394.
8 R. A. Wahaab, M. Mahmoud and J. B. van Lier, *Renew. Sustain. Energy Rev.*, 2020, **127**, 109880.
9 A. M. Othman, M. Mahmoud, M. Abdelraof, G. S. A. A. Karim and A. M. Elsayed, *Int. J. Biol. Macromol.*, 2021, **192**, 219–231.
10 Y. Li, B. Wu, G. Zhu, Y. Liu, W. J. Ng, A. Appan and S. K. Tan, *Sci. Total Environ.*, 2016, **562**, 604–613.

11 Y. He, A. A. M. Langenhoff, N. B. Sutton, H. H. M. Rijnaarts, M. H. Blokland, F. Chen, C. Huber and P. Schröder, *Environ. Sci. Technol.*, 2017, **51**, 4576–4584.
12 S. Chopra and D. Kumar, *Heliyon*, 2020, **6**, e04087.
13 V. A. Jiménez-Silva, F. Santoyo-Tepole, N. Ruiz-Ordaz and J. Galíndez-Mayer, *Process Saf. Environ. Prot.*, 2019, **123**, 140–149.
14 S. Lu, Y. Zhang, X. Liu, J. Xu, Y. Liu, W. Guo, X. Liu and J. Chen, *Ecotoxicol. Environ. Saf.*, 2021, **219**, 112292.
15 M. Mahmoud, P. Parameswaran, C. I. Torres and B. E. Rittmann, *RSC Adv.*, 2016, **6**, 6658–6664.
16 F. Mahmoudi, K. Saravanakumar, V. Maheskumar, L. K. Njaramba, Y. Yoon and C. M. Park, *J. Hazard. Mater.*, 2022, 129074.
17 H. Wang, Y. Wang and D. D. Dionysiou, *Water*, 2023, **15**, 398.
18 A. Pattnaik, J. N. Sahu, A. K. Poonia and P. Ghosh, *Chem. Eng. Res. Des.*, 2023, **190**, 667–686.
19 B. A. Mohamed, H. Hamid, C. V. Montoya-Bautista and L. Y. Li, *J. Clean. Prod.*, 2023, **389**, 136095.
20 M. P. Astuti, S. Notodarmojo, C. R. Priadi and L. P. Padhye, *Environ. Sci. Pollut. Res.*, 2023, **30**, 21512–21532.
21 D. Yadav, S. Rangabhashiyam, P. Verma, P. Singh, P. Devi, P. Kumar, C. M. Hussain, G. K. Gaurav and K. S. Kumar, *Chemosphere*, 2021, **272**, 129492.
22 T.-H. Le, C. Ng, N. H. Tran, H. Chen and K. Y.-H. Gin, *Water Res.*, 2018, **145**, 498–508.
23 L. Zhong, J. Ding, T. Wu, Y. Zhao, J. W. Pang, J.-P. Jiang, J.-Q. Jiang, Y. Li, N.-Q. Ren and S.-S. Yang, *J. Water Process Eng.*, 2023, **51**, 103389.
24 G. David, M. S. Rana, S. Saxena, S. Sharma, D. Pant and S. K. Prajapati, *Int. J. Environ. Sci. Technol.*, 2023, **20**, 9249–9270.
25 J. Li, L. Liu, Y.-M. Zheng, L. Ma, Q.-B. Zhao, X. Wang and C.-X. Liu, *Chem. Eng. J.*, 2023, **460**, 141619.
26 G. Sgrigna, C. Baldacchini, S. Dreveck, Z. Cheng and C. Calfapietra, *Sci. Total Environ.*, 2020, **718**, 137310.
27 Y. Deng, M. Zou, W. Liu, Y. Lian, Q. Guo, X. Zhang and A. Dan, *J. Clean. Prod.*, 2023, 136271.
28 P. Chen, X. Yu, J. Zhang and Y. Wang, *Front. Microbiol.*, 2023, **13**, 1110793.
29 M. Huong, D.-T. Costa and B. van Hoi, *Water Sci. Technol.*, 2020, **82**, 1995–2006.
30 X. Li, W. Zhu, G. Meng, C. Zhang and R. Guo, *J. Environ. Manage.*, 2020, **273**, 111120.
31 Y. Yuan, B. Yang, H. Wang, X. Lai, F. Li, M. M. A. Salam, F. Pan and Y. Zhao, *Bioresour. Technol.*, 2020, **310**, 123419.
32 F. Liu, Y. Zhang and T. Lu, *Process Saf. Environ. Protect.*, 2023, **169**, 293–303.
33 S. Gupta, A. Patro, Y. Mittal, S. Dwivedi, P. Saket, R. Panja, T. Saeed, F. Martínez and A. K. Yadav, *Sci. Total Environ.*, 2023, **879**, 162757.
34 X. Liu, S. Lu, Y. Liu, Y. Wang, X. Guo, Y. Chen, J. Zhang and F. Wu, *Water Res.*, 2021, **207**, 117814.
35 M. Jain, P. S. Kiran, P. S. Ghosal and A. K. Gupta, *J. Environ. Manag.*, 2023, **344**, 118686.
36 X. Wang, Y. Tian, H. Liu, X. Zhao and S. Peng, *Sci. Total Environ.*, 2019, **653**, 860–871.
37 M. Hartl, M. J. García-Galán, V. Matamoros, M. Fernández-Gatell, D. P. L. Rousseau, G. D. Laing, M. Garfí and J. Puigagut, *Chemosphere*, 2021, **271**, 129593.
38 M. Mahmoud, P. Parameswaran, C. I. Torres and B. E. Rittmann, *Biotechnol. Bioeng.*, 2017, **114**, 1151–1159.
39 APHA, *Standard methods for the examination of water and wastewater*, American Public Health Association (APHA), Washington, DC, USA, 2005.
40 M. Mahmoud and K. M. El-Khatib, *Int. J. Hydrogen Energy*, 2020, **45**, 32413–32422.
41 D. Z. Khater, R. S. Amin, M. O. Zhran, Z. K. Abd El-Aziz, M. Mahmoud, H. M. Hassan and K. M. El-Khatib, *J. Genet. Eng. Biotechnol.*, 2022, **20**, 12.
42 L. Zhang, T. Lv, Y. Zhang, O. R. Stein, C. A. Arias, H. Brix and P. N. Carvalho, *Sci. Total Environ.*, 2017, **609**, 38–45.
43 M. Mahmoud, A. S. El-Kalliny and G. Squadrito, *Energy Convers. Manag.*, 2022, **254**, 115225.
44 M. Mahmoud, C. I. Torres and B. E. Rittmann, *Environ. Sci. Technol.*, 2017, **51**, 13461–13470.
45 B. Ji, Y. Zhao, J. Vymazal, Ü. Mander, R. Lust and C. Tang, *Chemosphere*, 2021, **262**, 128366.
46 S. Gupta, P. Srivastava, S. A. Patil and A. K. Yadav, *Bioresour. Technol.*, 2021, **320**, 124376.
47 S. Luo, Z.-Y. Zhao, Y. Liu, R. Liu, W.-Z. Liu, X.-C. Feng, A.-J. Wang and H.-C. Wang, *Chem. Eng. J.*, 2023, **457**, 141133.
48 H. Li, S. Zhang, X.-L. Yang, Y.-L. Yang, H. Xu, X.-N. Li and H.-L. Song, *Chemosphere*, 2019, **217**, 599–608.
49 S. Zhang, H.-L. Song, X.-L. Yang, Y.-L. Yang, K.-Y. Yang and X.-Y. Wang, *RSC Adv.*, 2016, **6**, 95999–96005.
50 H. Li, H. Xu, H.-L. Song, Y. Lu and X.-L. Yang, *Environ. Pollut.*, 2020, **265**, 115084.
51 M. Dai, Y. Zhang, Y. Wu, R. Sun, W. Zong and Q. Kong, *J. Environ. Chem. Eng.*, 2021, **9**, 106193.
52 H. Li, H. Xu, Y.-L. Yang, X.-L. Yang, Y. Wu, S. Zhang and H.-L. Song, *Water Res.*, 2019, **165**, 114988.
53 M. Dai, Y. Wu, J. Wang, Z. Lv, F. Li, Y. Zhang and Q. Kong, *Chemosphere*, 2022, **305**, 135377.
54 H. Wen, H. Zhu, Y. Xu, B. Yan, B. Shutes, G. Bañuelos and X. Wang, *Environ. Pollut.*, 2021, **272**, 115988.
55 L. Doherty, Y. Zhao, X. Zhao, Y. Hu, X. Hao, L. Xu and R. Liu, *Water Res.*, 2015, **85**, 38–45.
56 J. Wang, X. Song, Y. Wang, J. Bai, M. Li, G. Dong, F. Lin, Y. Lv and D. Yan, *Sci. Total Environ.*, 2017, **607**, 53–62.
57 L. Lu, D. Xing and N. Ren, *Water Res.*, 2012, **46**, 2425–2434.
58 A. Oodally, M. Gulamhussein and D. G. Randall, *J. Water Process Eng.*, 2019, **32**, 100930.
59 P. Srivastava, S. Dwivedi, N. Kumar, R. Abbassi, V. Garaniya and A. K. Yadav, *Bioresour. Technol.*, 2017, **244**, 1178–1182.
60 H. Li, K. Wang, J. Xu, H. Wu, Y. Ma, R. Zou and H.-L. Song, *Chemosphere*, 2023, 139461.
61 M. Salah, Y. Zheng, Q. Wang, C. Li, Y. Li and F. Li, *Sci. Total Environ.*, 2023, 163721.
62 Y.-J. Choi, L.-H. Kim and K.-D. Zoh, *Ecol. Eng.*, 2016, **91**, 85–92.
63 H. Ilyas, I. Masih and E. D. van Hullebusch, *J. Water Health*, 2020, **18**, 253–291.

64 M. El-Qelish and M. Mahmoud, *Sci. Total Environ.*, 2022, **802**, 149851.
65 Y. Liang, H. Zhu, G. Bañuelos, B. Shutes, B. Yan and X. Cheng, *Chem. Eng. J.*, 2018, **341**, 462–470.
66 J. Wang, X. Song, Y. Wang, J. Bai, M. Li, G. Dong, F. Lin, Y. Lv and D. Yan, *Sci. Total Environ.*, 2017, **607**, 53–62.
67 D. Z. Khater, R. S. Amin, M. Mahmoud and K. M. El-Khatib, *RSC Adv.*, 2022, **12**, 2207–2218.
68 N. Saeidi, F. Harnisch, V. Presser, F.-D. Kopinke and A. Georgi, *Chem. Eng. J.*, 2023, 144354.
69 Y. Kong, W. Li, Z. Wang, C. Yao and Y. Tao, *Electrochem. Commun.*, 2013, **26**, 59–62.
70 W. Yang, H. Han, M. Zhou and J. Yang, *RSC Adv.*, 2015, **5**, 49513–49520.
71 T. Scheytt, P. Mersmann, R. Lindstädt and T. Heberer, *Water, Air, Soil Pollut.*, 2005, **165**, 3–11.
72 O. E. Ohore, Z. Qin, E. Sanganyado, Y. Wang, X. Jiao, W. Liu and Z. Wang, *J. Hazard. Mater.*, 2022, **424**, 127495.
73 S. Mathews and D. Reinhold, *Environ. Sci. Pollut. Res.*, 2013, **20**, 4327–4338.
74 X. Zhou, X. Zhang, Y. Peng, A. I. Douka, F. You, J. Yao, X. Jiang, R. Hu and H. Yang, *Molecules*, 2023, **28**, 4372.
75 T. Yamada, Y. Sekiguchi, H. Imachi, Y. Kamagata, A. Ohashi and H. Harada, *Appl. Environ. Microbiol.*, 2005, **71**, 7493–7503.
76 G. L. Garbini, A. B. Caracciolo and P. Grenni, *Microorganisms*, 2023, **11**, 1255.
77 K. Jawaharraj, N. Shrestha, G. Chilkoor, B. Vemuri and V. Gadhamshetty, *Bioelectrochemistry*, 2020, **135**, 107549.
78 Q. Feng, L. Xu, C. Liu, H. Wang, Z. Jiang, Z. Xie, Y. Liu, Z. Yang and Y. Qin, *J. Clean. Prod.*, 2020, **269**, 121776.